Original Research (2026) 3(2); 17 - 26
https://doi.org/10.22103/VCBR.2025.24819.1046

Shahid Bahonar University of Kerman

Veterinary and Comparative Biomedical Research

ORIGINAL ARTICLE

A Comprehensive Computed Tomographic Anatomy of the Mediastinal Cavity in Jebeer (*Gazella bennettii*)

Seyed Mohsen Sajjadian [1*], Bahador Shojaei [1], Darioush Vosough [2], Babak Filolahi [3], Masoud Abedi [3]

[1] *Department of Basic Sciences, Faculty of Veterinary Medicine, Shahid Bahonar University of Kerman, Kerman, Iran*
[2] *Department of Clinical Sciences, Faculty of Veterinary Medicine, Shahid Bahonar University of Kerman, Kerman, Iran*
[3] *Faculty of Veterinary Medicine, Shahid Bahonar University of Kerman, Kerman, Iran*

Online ISSN: 3060-7663 **https://doi.org/10.22103/VCBR.2025.24819.1046**

***Correspondence**

Author's Email:
Sajjadian@uk.ac.ir

Article History

Received: *12 February 2025*
Revised: *29 March 2025*
Accepted: *21 April 2025*
Published: *17 May 2025*

Keywords

Computed tomography
Anatomy
Mediastinal cavity
Jebeer
Gazella bennettii

Abstract

Jebeer (*Gazella bennettii*) primarily inhabits the central and southeastern regions of Iran. The estimated population in this country is only around 1,300 individuals, underscoring the need for increased conservation efforts and research. Due to the lack of anatomical data for this species and to address urgent conservation needs, such as veterinary care, this study aimed to provide detailed anatomical insights into the mediastinal cavity of the Jebeer using non-invasive computed tomography (CT). Four healthy adult Jebeer, both males and females, aged 2.5 - 3.5 years and weighing 20–25 kg were anesthetized and positioned in sternal recumbency. CT images of the thoracic region were acquired perpendicular to the thoracic vertebrae, with a slice thickness of 3 mm. Thoracic vertebrae served as anatomical landmarks to describe the position and extent of mediastinal organs. Structures were compared to those of dissected goats for reference. Key structures such as the trachea, cranial vena cava, and aorta in Jebeer exhibited similarities to the corresponding landmarks in goats. The trachea bifurcated at the level of the 6th thoracic vertebra, while the cranial vena cava entered the right atrium at the 4th thoracic vertebra. The aortic arch and pulmonary trunk were observed at the 4th-5th and 6th thoracic vertebrae, respectively. No anatomical differences were observed between males and females in the mediastinal structures. Species-specific variations in the positioning of pulmonary vessels and other structures were identified when compared to other ruminants and carnivores. Additionally, the angle and position of the heart in the Jebeer were distinct from those in carnivores, resulting in differences in the attachment sites of the major blood vessels. This research provides a comprehensive CT-based anatomical atlas of the mediastinal cavity in the Jebeer, offering valuable insights for veterinary diagnostics and treatment of mediastinal conditions. These findings can also support targeted conservation strategies for this endangered species.

How to cite this article: Seyed Mohsen Sajjadian, Bahador Shojaei, Darioush Vosough, Babak Filolahi, Masoud Abedi. A Comprehensive Computed Tomographic Anatomy of the Mediastinal Cavity in Jebeer (*Gazella bennettii*). *Veterinary and Comparative Biomedical Research*, 2026, 3(2): 17 – 26. http://doi:10.22103/VCBR.2025.24819.1046

Introduction

Jebeer (*Gazella bennettii*) is a species of the genus *Gazella* that primarily inhabits the central and southeast regions of Iran (1-3). The Jebeer's habitat is primarily in arid regions, where it has adapted to survive with minimal water availability. This adaptation is critical given the ecological pressures the species faces due to habitat loss and hunting. Although the species is fully protected by the law, only around 1,300 individuals are estimated for this country, indicating a need for greater attention. Conservationists emphasize the importance of protecting these gazelles for their intrinsic value and for maintaining ecological balance within their habitats (4). The decline in population highlights the urgent need for enhanced conservation efforts and research initiatives focused on this species and its habitat (5). Due to the lack of anatomical studies on Jebeer (6, 7), this study aimed to prepare detailed anatomical images of the mediastinum of this endangered species using the noninvasive computed tomography (CT) technique.

The mediastinum, the central compartment of the thoracic cavity, houses critical structures such as the heart, major vessels, trachea, bronchi, esophagus, thymus, and lymph nodes. Accurate imaging of this region is essential for diagnosing a wide range of pathological conditions, including neoplasia, vascular anomalies, inflammatory masses, and trauma-related injuries. In veterinary medicine, CT has become an indispensable diagnostic tool for evaluating intra-thoracic structures due to its ability to provide detailed cross-sectional images without the superimposition inherent to traditional radiography (8, 9). This imaging technique enables the examination of body cross-sections in live animals. Modern multi-detector CT scanners routinely image patients ranging from small pets to large species, including horses (10). In addition to neoplasia, CT in dogs and cats is used for a variety of thoracic problems (11, 12). CT enables non-invasive cross-sectional imaging of the thorax, overcoming the structural overlap seen on standard radiographs. It provides superior contrast for solid, fatty, cystic, calcified, and vascular tissues. In dogs and cats, CT is now considered the second-tier imaging modality after radiographs for thoracic evaluation. CT offers unparalleled detail of thoracic pathology in pets, from airway foreign bodies to occult mediastinal lymphadenopathy. It is also a valuable tool for assessing intra-thoracic diseases and allowing for improved diagnosis of the presence, location, and extension of pathology and involvement of thoracic structures compared to standard radiography (8-10). While CT has been predominantly utilized for diagnostic purposes in small animals (8, 9, 13-17), its application has expanded to include non-invasive studies in larger animals. In Equine veterinary practice, CT is increasingly employed, especially for imaging the skull and limbs, and this technology is becoming more accessible. For equine species, whole-body mediastinal CT is limited by size, but specialized scans of the head and extremities are commonplace (18). Reports indicate a growing trend in employing CT to identify mass-filled abnormalities (19-21), assess tissue volumes, and manage fractures in large herbivores (22-24). Recent studies on the abdominal cavity of Jebeer have utilized spiral CT imaging to precisely illustrate internal organs without requiring invasive procedures (25-41). CT imaging offers clear and detailed views of these animals' anatomical structures, enhancing understanding of their biology and supporting the development of effective conservation strategies to protect their populations and habitats. This study aims to advance knowledge of the mediastinum in Jebeer using noninvasive CT imaging. This method improves veterinary practices by facilitating better diagnosis and treatment of mediastinal conditions while providing important anatomical information to identify potential diseases.

Materials and methods

Four healthy adult males and females, Jebeer, weighing approximately 20-25 kg and aged 2.5-3.5 years, were obtained through collaboration with the Kerman Provincial Environmental Organization under the supervision of the organization's designated veterinarian. Each Jebeer received intramuscular Atropine (Daroopakhsh, Iran) at a dosage of 0.04 mg/kg to reduce salivary and respiratory secretions and to counteract xylazine-induced bradycardia. Then anesthetized by intravenous injection of mixed 10% Ketamine (Alfasan, The Netherlands) at 2.2 mg/kg and 2% Xylazine (Alfasan, The Netherlands) at 0.11 mg/kg. The dosages of anesthetic agents were adapted from established protocols for small ruminants and adjusted to account for anatomical and physiological similarities between *Gazella bennettii* and this taxonomic group. The Jebeers were positioned in sternal recumbency, and X-ray radiation was adjusted at an angle of 90 degrees to the longitudinal axis of the trunk. Tomograms were acquired at a thickness of 3 mm using a third-generation CT scanner with dynamic scanning capabilities (Toshiba X-Vision EX, Japan). The acquisition parameters were KVp 120, mA 100, and a scan time of 1 second. Window width and level were adjusted as necessary to obtain the optimal image of the thoracic organs (WW: 415 and WL: 28).

Following image acquisition, two goats-selected as a comparative anatomical model, to the best of the authors'

knowledge, based on the anatomical similarities between Jebeer gazelles (*Gazella bennettii*) and small ruminants-were euthanized with an overdose of pentobarbital while still under anesthesia. CT images were labeled by comparison with the dissected thorax of the euthanized goats. Thoracic vertebrae were used as landmarks to describe the location and extension of the thoracic organs.

Table 1. Topographical position of mediastinal organs in Jebeer according to the thoracic vertebrae

Mediastinal organs	T1	T2	T3	T4	T5	T6	T7	T8	T9	T10
Trachea	+	+	+	+	+					
Esophagus	+	+	+	+	+	+	+	+	+	+
Brachiocephalic trunk	+	+	+	+						
Cranial vena cava	+	+	+	+						
Bi carotid trunk	+									
Right subclavian artery	+									
Costo-cervical vein				+						
Right azygos vein				+						
Left subclavian artery		+								
Right atrium					+	+	+			
Right ventricle					+	+	+			
Aortic arch					+					
Descending aorta						+	+	+	+	+
Pulmonary trunk						+				
Right and left pulmonary arteries							+			
Tracheal bifurcation						+				
Left atrium							+	+		
Left ventricle							+	+	+	
Pulmonary vein								+		
Left azygos vein							+	+	+	
Caudal vena cava							+	+	+	+
Caudal mediastinal lymph node								+	+	+

Results

In Figures 1 to 13, CT images selected from one Jebeer are viewed from cranial to caudal. Transverse images illustrate the animal's left and dorsal aspects on the left and top sides of the images, respectively. The selected images were achieved from the first to the tenth thoracic vertebrae; subsequently, the positions of mediastinal organs were evaluated relative to adjacent vertebrae (Table 1).

The trachea entered the mediastinum medial to the right first rib and lies on the right side of the esophagus (Figure 1). It is separated from the right thoracic wall by the apical lobe of the right lung (Figure 2). In the cranial half of the cranial mediastinum, the trachea was located in the dorsal half of the thoracic cavity (Figures 1 and 2). However, as the vertical diameter increased within this cavity, it gradually displaced towards the dorsal third of the mediastinum (Figure 3). The trachea coursed caudally to the level of the sixth thoracic vertebra (Figure 9), bifurcating dorsal to the heart base into right and left bronchi (Figure 10).

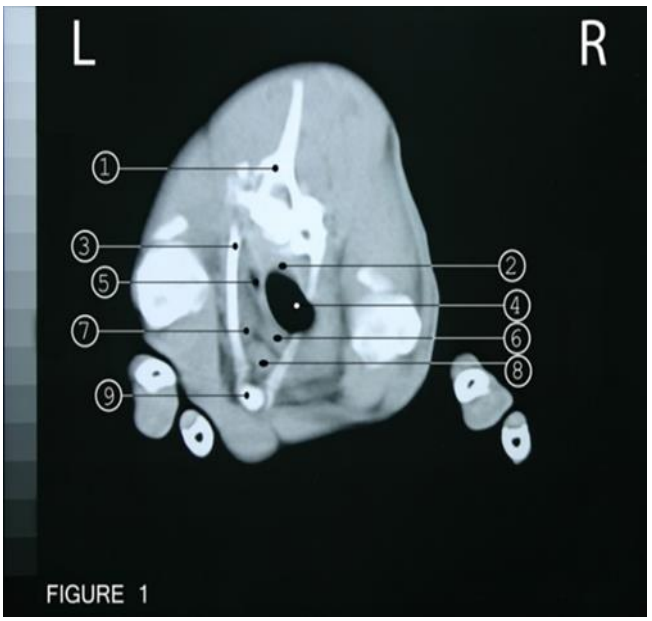

Figure 1. 1. 1st thoracic vertebra, 2. longus colli muscle, 3. 1st rib, 4. trachea, 5. esophagus, 6. right subclavian artery, 7. bicarotid trunk, 8. jugular vein

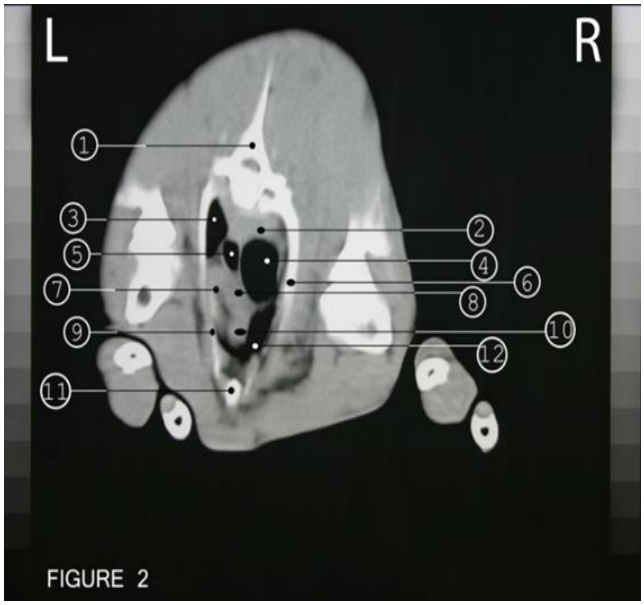

Figure 2. 1. 2nd thoracic vertebra, 2. longus colli muscle, 3. left lung, 4. trachea, 5. esophagus, 6. 2nd rib, 7. left subclavian artery, 8. brachiocephalic trunk, 9. 1st rib, 10. cranial vena cava, 11. sternum, 12. right lung

The cranial vena cava (Figures 2 to 6) was formed by the union of two external jugular veins at the level of 1st thoracic vertebra. It was seen first ventral to the brachiocephalic trunk, but beyond the caudal part of the 2nd thoracic vertebra, it gradually displaced to the right side of the mentioned artery. Along its course, it was seen as a round structure in all images from the caudal part of the 1st to the caudal part of the 4th thoracic vertebrae, which entered the right atrium (Figure 6).

The aortic arch was observed along the caudal part of the 4th to 5th thoracic vertebrae as a relatively vertical structure positioned to the left of the junction of the cranial vena cava with the heart (Figures 6 and 7). At the level of the 4th thoracic vertebra, it detached the brachiocephalic trunk cranially as a round structure left to the cranial vena cava (Figure 6). The brachiocephalic trunk was situated ventral to the esophagus in the cranial mediastinum, extending along the first four thoracic vertebrae (Figures 1 to 6). The right and left subclavian arteries branched from the brachiocephalic trunk at the level of the 1st and 2nd thoracic vertebrae (Figures 1 and 2). The descending aorta (Figures 9 to 13) was identified dorsal to the base of the heart and to the left side of the esophagus at the level of the caudal part of 6th thoracic vertebra (Figure 9). It shifted dorsally within the caudal mediastinum during its caudal course and was situated dorsal to the esophagus and ventral to the longus colli muscles between 6th and 7th thoracic vertebrae. From the 7th thoracic vertebrae caudally, where the longus colli muscles disappeared, the aorta was observed directly beneath the vertebral bodies (Figures 10 to 13).

The pulmonary trunk was observed continuing from the conus arteriosus, positioned beneath the descending aorta at the level of the 6th thoracic vertebra (Figure 9). It coursed a short distance caudally to the level of the caudal part of this vertebra, where it bifurcated into the right and left pulmonary arteries (Figure 10).

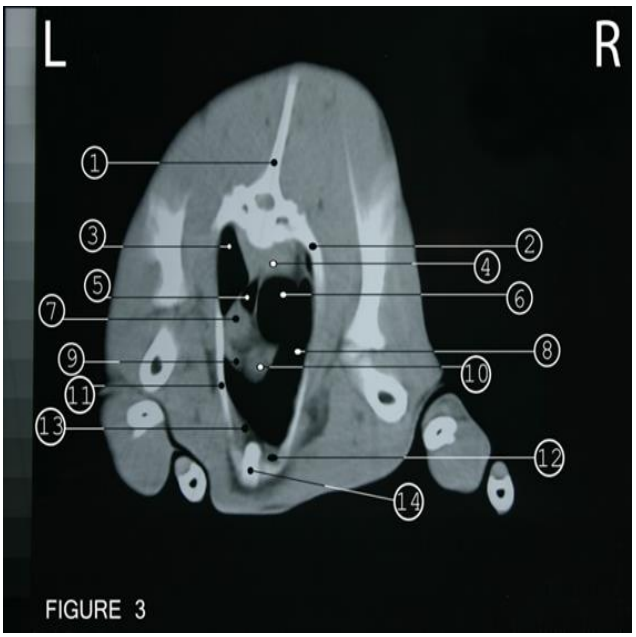

Figure 3. 1. 3rd thoracic vertebra, 2. 3rd rib, 3. left lung, 4. longus colli muscle, 5. esophagus, 6. trachea, 7. brachiocephalic trunk, 8. right lung, 9. mediastinal mass, 10. cranial vena cava, 11. 2nd rib, 12. internal thoracic vessels, 13. transverse thoracic muscle, 14. sternum

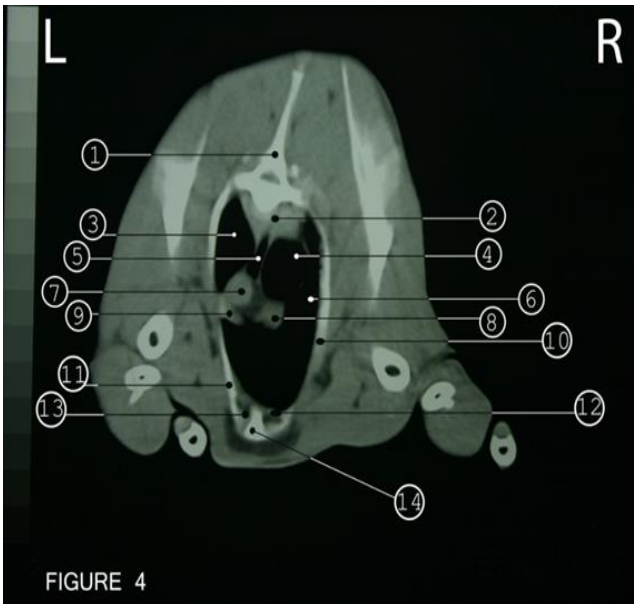

Figure 4. 1. 3rd thoracic vertebra, 2. longus colli muscle, 3. left lung, 4. trachea, 5. esophagus, 6. right lung, 7. brachiocephalic trunk, 8. cranial vena cava, 9. mediastinal mass, 10. 3rd rib, 11. 2nd rib, 12. transverse thoracic muscle, 13. internal thoracic vessels, 14. sternum

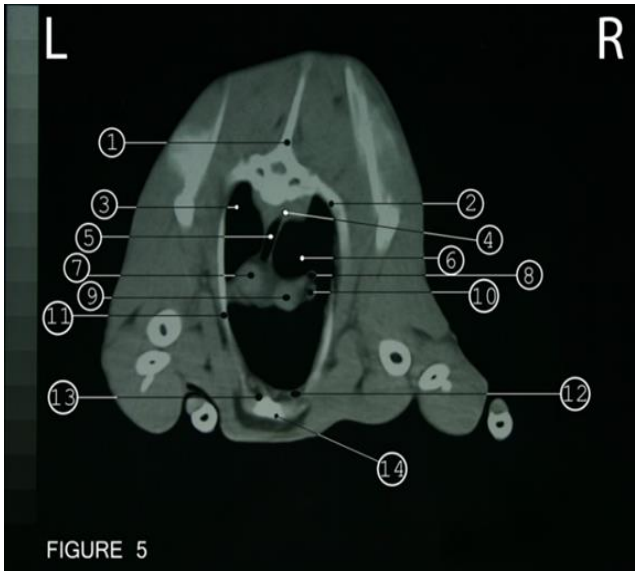

Figure 5. 1. 4th thoracic vertebra, 2. 4th rib, 3. left lung, 4. longus colli muscle, 5. esophagus, 6. trachea, 7. brachiocephalicus trunk, 8. costocervical vein, 9. cranial vena cava, 10. right azygos, 11. 3rd rib, 12. transverse thoracis muscle, 13. internal thoracic vessels, 14. sternum

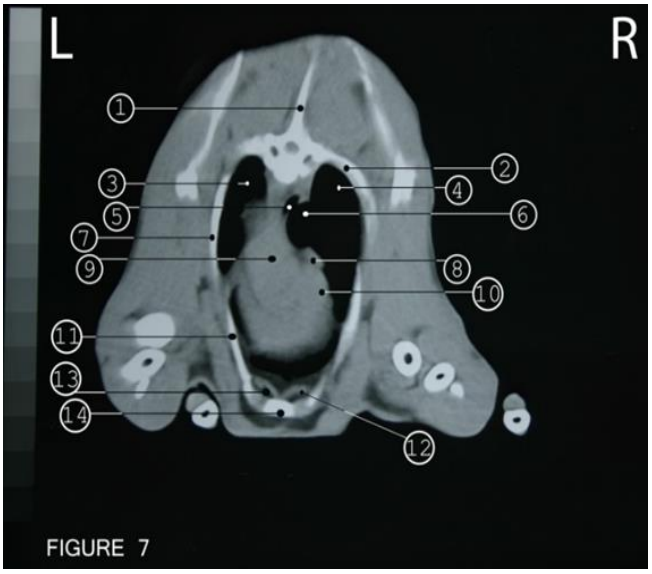

Figure 7. 1. 5th thoracic vertebra, 2. 5th rib, 3. left lung, 4. right lung, 5. esophagus, 6. trachea, 7. 4th rib, 8. pulmonary vessels, 9. aortic arch, 10. right atrium, 11. 3rd rib, 12. transverse thoracis muscle, 13. internal thoracic vessels, 14. sternum

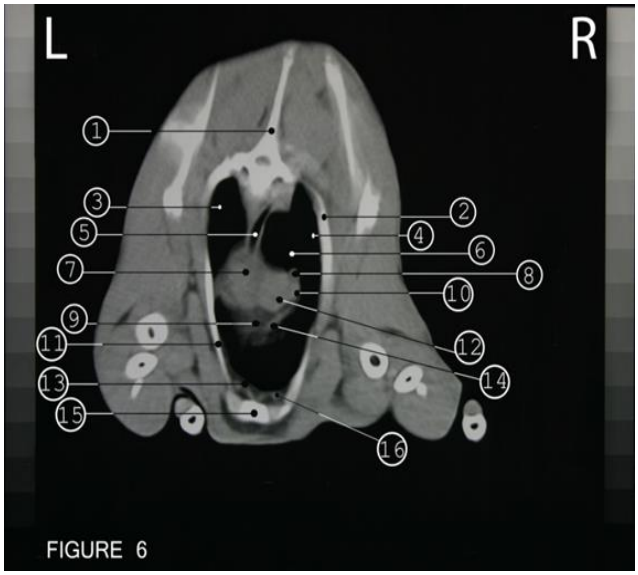

Figure 6. 1. 4th thoracic vertebra, 2. 4th rib, 3. left lung, 4. right lung, 5. esophagus, 6. trachea, 7. brachiocephalic trunk, 8. costocervical vein, 9. cranial border of heart, 10. right azygos, 11. 3rd rib, 12. cranial vena cava, 13. transverse thoracic muscle, 14. right atrium, 15. sternum, 16. internal thoracic vessels

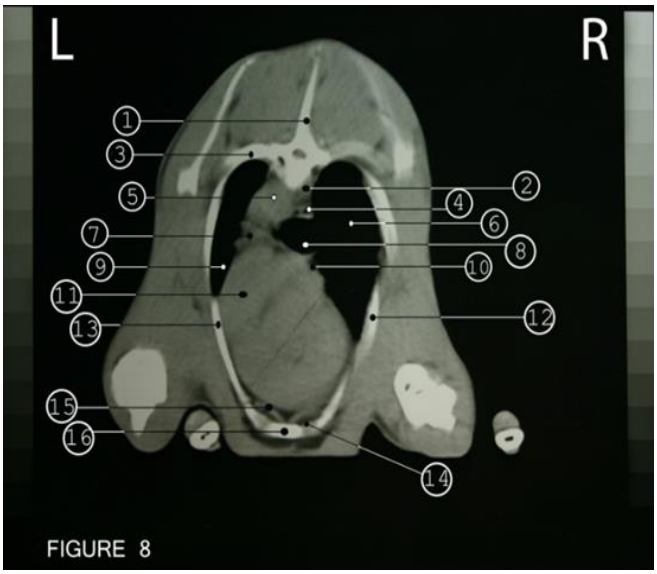

Figure 8. 1. 6th thoracic vertebra, 2. longus colli muscle, 3. 6th rib, 4. esophagus, 5. descending aorta, 6. right lung, 7. pulmonary trunk, 8. tracheal bifurcation, 9. left lung, 10. pulmonary vessels, 11. conus arteriosus, 12. 5th rib, 13. 4th rib, 14. internal thoracic vessels, 15. transverse thoracic muscle, 16. sternum

At the level of the 8th thoracic vertebra, the pulmonary veins converged to meet the heart at the midline (Figure 11). Caudal to this point, they diverged to form distinct right and left pulmonary veins, which were observed medial to their respective pulmonary arteries (Figure 12).

The internal thoracic veins were positioned medially to their corresponding arteries; these vessels were observed along the 3rd to 10th thoracic vertebrae (Figures 3 to 13). The costo-cervical and right azygos veins (Figures 5 and 6) entered the cranial vena cava at the level of the 4th thoracic vertebra, respectively. The left azygos vein was observed just beneath the left side of the descending aorta between the 7th and 9th thoracic vertebrae (Figures 10 to 12).

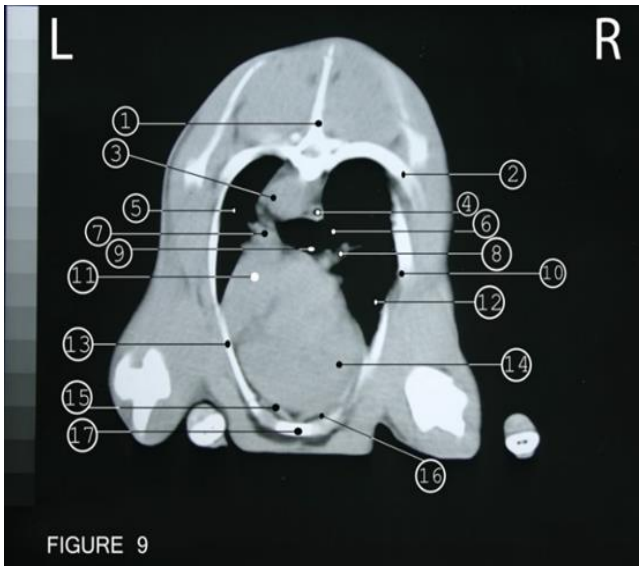

Figure 9. 1. 7th thoracic vertebra, 2. 7th rib, 3. descending aorta, 4. esophagus, 5. left lung, 6. right bronchus, 7. left pulmonary artery, 8. right pulmonary artery, 9. left bronchus, 10. 6th rib, 11. right ventricle, 12. right lung, 13. 5th rib, 14. left ventricle, 15. transverse thoracis muscle, 16. internal thoracic vessels, 17. sternum

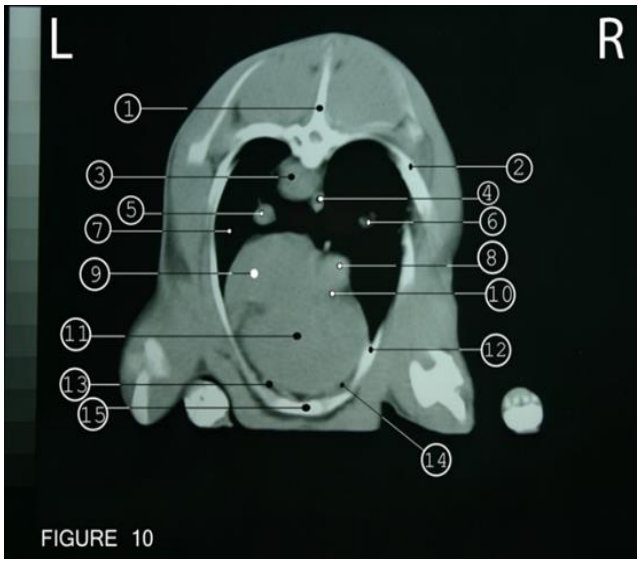

Figure 10. 1. 7th thoracic vertebra, 2. 7th rib, 3. descending aorta, 4. esophagus, 5. caudal branch of the left pulmonary artery, 6. caudal branch of the right pulmonary artery, 7. left lung, 8. caudal vena cava, 9. left atrium, 10. right atrium, 11. left ventricle, 12. 5th rib, 13. internal thoracic vessels, 14. transverse thoracic muscle, 15. sternum

Discussion

This study expands the anatomical knowledge of the endangered Jebeer (*Gazella bennettii*) by providing a detailed CT atlas of the mediastinal cavity, a region previously underexplored in this species. The results delineate the spatial relationships of mediastinal structures, such as the trachea, cranial vena cava, aortic arch, and pulmonary trunk, relative to thoracic vertebral landmarks. Key observations include tracheal bifurcation at the 6th thoracic vertebra, the cranial vena cava's entry into the right atrium at the 4th vertebra, and species-specific variations in pulmonary vessel positioning and cardiac angulation compared to goats. These findings complement prior anatomical studies on Jebeer and address a critical gap in understanding mediastinal anatomy in this species.

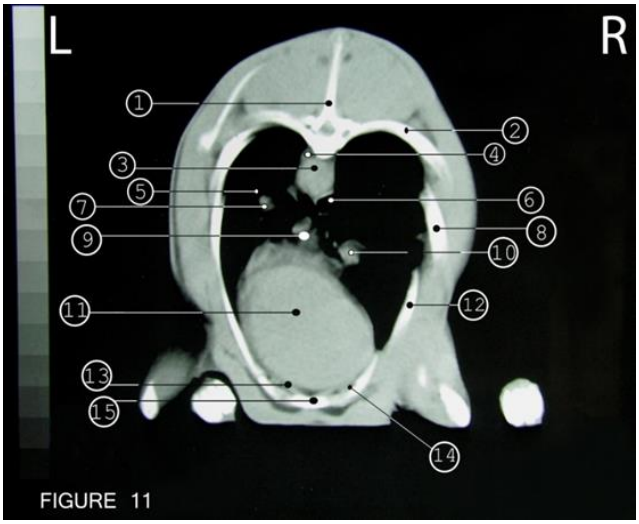

Figure 11. 1. 8th thoracic vertebra, 2. 8th rib, 3. descending aorta, 4. left azygos, 5. left lung, 6. esophagus, 7. caudal branch of the left pulmonary artery, 8. 7th rib, 9. pulmonary veins, 10. caudal vena cava, 11. left ventricle, 12. 6th rib, 13. transverse thoracic muscle, 14. internal thoracic vessels, 15. sternum

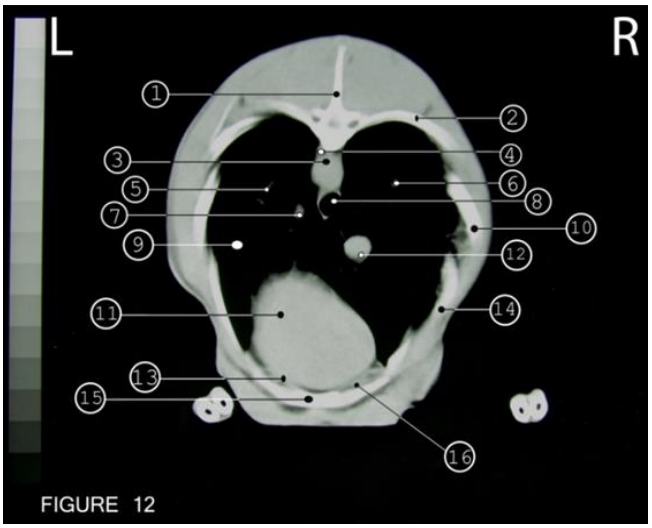

Figure 12. 1. 9th thoracic vertebra, 2. 9th rib, 3. descending aorta, 4. left azygos, 5. caudal branch of the left pulmonary artery, 6. caudal branch of the right pulmonary artery, 7. caudal branch of pulmonary veins, 8. esophagus, 9. left lung, 10. 8th rib, 11. left ventricle, 12. caudal vena cava, 13. transverse thoracic muscle, 14. internal thoracic vessels, 15. sternum

While earlier CT studies focused on the Jebeer's bronchial tree, nasal cavity, and abdominal organs (6, 7, 41), this work uniquely bridges the gap in understanding thoracic anatomy. The distinct cardiac orientation and vascular topography, differing from both goats and carnivores, suggest adaptive anatomical traits that may optimize cardiopulmonary function in arid environments. Clinically, these insights refine diagnostic criteria for mediastinal pathologies (e.g., masses, vascular anomalies) and underscore the need for species-specific reference standards in veterinary imaging.

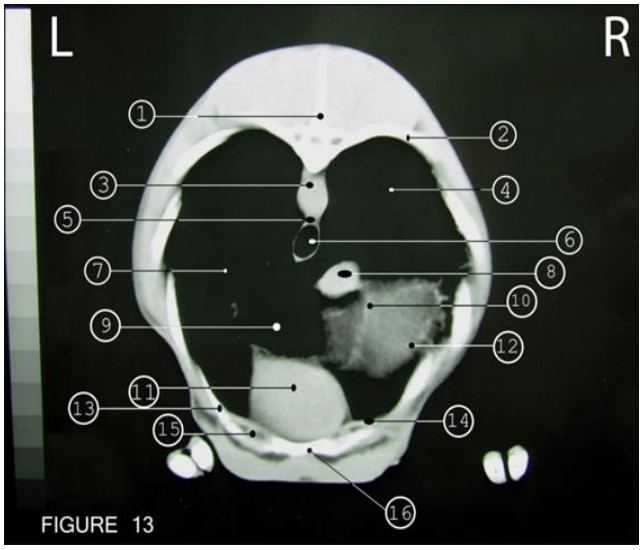

Figure 13. 1. 10th thoracic vertebra, 2. 10th rib, 3. descending aorta, 4. right lung, 5. caudal mediastinal lymph node, 6. esophagus, 7. left lung, 8. caudal vena cava, 9. reticulum, 10. right cranial phrenic vein, 11. apex of heart, 12. liver, 13. 6th rib, 14. transverse thoracic muscle, 15. internal thoracic vessels, 16. sternum

In the present study, thoracic vertebrae were used as a reference to describe the topographical position of mediastinal organs. Normal CT features of the thoracic cavity of small animals have been studied in recent years (31, 32, 34, 37). However, only a few articles have focused on the CT anatomy of the ruminants (6, 7, 27, 29, 38, 39). These include a study by Alston et al. (2009), which examined CT imaging for assessing tissue volume in sheep and demonstrated that similar techniques can provide valuable insights into different ruminant species (20). Additionally, research by Arencibia et al. (1997) showed that CT could effectively delineate cranio-encephalic structures in goats, further supporting the utility of advanced imaging techniques in veterinary anatomy (27). Our study addresses this gap by preparing a sectional imaging anatomical atlas of the thoracic organs in the Jebeer. This atlas facilitates understanding the situation and extension of these organs relative to the vertebral column (Table 1).

The trachea, cranial vena cava, esophagus, and brachiocephalic trunk were observed in the same position in the cranial mediastinum as described by Shojaei et al. (2012) in Rayini goats. We also observed descending aorta and pulmonary artery bifurcation in one vertebra caudal to the positions reported in the mentioned study (42), consistent with findings by Alsafy (2008) in goats (40). This observation aligns with findings from Patsikas et al. (2001), who noted variations in vascular anatomy among different ruminant species (15).

The observed differences in the topography and angulation of the Jebeer's heart, along with the distinct positioning of its proximal vasculature, highlight critical interspecies anatomical variations when compared to carnivores such as dogs and cats (31, 34, 37, 43, 44).

If the position and course of the cranial vena cava described in this study are disregarded, mislabeling may occur (40). In young animals, the brachiocephalic trunk, bicarotid trunk, and thymus may be confused with the cranial vena cava. Hahn et al. (1990) previously noted this potential for confusion in discussions of vascular anatomy in small animals (13). Differential identification of the caudal vena cava and right pulmonary artery can be achieved by noting the former vessel's greater diameter and more ventral position.

According to the anatomy of the right azygos and costo-cervical veins (42-44), these two veins were detected at their entrance to the cranial vena cava at the level of the 4th thoracic vertebra in the cranial mediastinum, respectively. This finding is consistent with observations made by Diana et al. (2006), who also identified similar anatomical landmarks in small animal thoracic anatomy (8).

The right and left transverse thoracic muscles served as appropriate landmarks for identifying the underlying internal thoracic vessels, which were observed from the 3rd to 10th thoracic vertebrae in this study. The more cranial location of the pulmonary trunk bifurcation compared to the incorporation of the caudal vena cava into the right atrium (31, 34, 42), helps prevent mislabeling of these vessels. The left pulmonary artery and vein were observed closer to the median plane than the right vessels, supporting previous studies that indicate asymmetrical positioning of pulmonary vessels based on species-specific anatomy (20). These vessels are positioned dorsal to the level of the caudal vena cava. The pulmonary veins were also positioned more medially than the corresponding arteries. This mediastinal atlas enhances veterinary care by enabling precise localization of thoracic structures during imaging or surgical interventions. For conservationists, it

provides a baseline for monitoring cardiopulmonary health in captive breeding programs, which are critical for this endangered species. The non-invasive CT approach also models ethical research practices by minimizing stress on vulnerable populations. Furthermore, the study underscores the value of incremental anatomical research-each focused study (nasal, abdominal, and now mediastinal) collectively builds a holistic understanding of the species, informing both conservation and clinical strategies.

While the study benefits from CT imaging of live Jebeer specimens, thereby avoiding post-mortem positional artifacts, several constraints remain. The small sample size (n=4) limits the assessment of individual or demographic (age/sex) variability in mediastinal anatomy. Furthermore, anesthesia itself may alter physiological parameters (e.g., respiratory depth, cardiac output), subtly influencing vascular or tracheal dimensions. Finally, comparisons with dissected goats, though pragmatically necessary, introduce methodological asymmetry, as post-mortem tissue changes in goats (e.g., loss of vascular tone, gravitational shifts) may skew anatomical correlations. These limitations underscore the need for larger-scale live-animal studies to validate findings under more ecologically relevant conditions, ideally incorporating dynamic or standing CT protocols. Future studies should increase sample sizes to assess demographic variability and employ dynamic CT protocols to evaluate posture-dependent anatomical shifts, such as imaging in standing or locomoting Jebeer Cross-species comparisons within the *Gazella* genus may reveal adaptive trends tied to environmental pressures. Linking anatomical findings to ecological data-such as thermoregulation strategies or foraging efficiency-could elucidate evolutionary drivers behind observed traits, bridging anatomical research with conservation-driven field studies.

Conclusion

Though not the first CT study on Jebeer, this work represents a pivotal advancement in mediastinal anatomy by addressing a critical void in the existing literature. Synthesizing vertebral landmarks, species-specific variations, and clinical relevance, the study equips veterinarians and conservationists with actionable insights. As anthropogenic pressures threaten the Jebeer's survival, such anatomical precision becomes indispensable for informed conservation and healthcare, exemplifying how iterative research fosters both species preservation and scientific progress.

Acknowledgements

The Research Council of Shahid Bahonar University of Kerman, Iran, financially supported this research. The authors thank the Environmental Department of Kerman for providing the necessary research conditions and granting animal access. Additionally, they thank Dr. Madjid Tahmoresi for his valuable contributions to the computed tomography aspect of this study.

Authors' Contributions

Seyed Mohsen Sajjadian: Conceptualization, Data Curation, Formal analysis, Investigation, Methodology, Supervision, Validation, Visualization, Writing – original draft, Writing – review & editing. **Bahador Shojaei:** Conceptualization, Project Administration, Methodology, Supervision, Investigation (CT Imaging & Data Acquisition), Formal Analysis, Data Curation, Writing – original draft, Writing – Review & Editing. **Darioush Vosough:** Formal analysis, Investigation, Methodology, Supervision. **Babak Filolahi:** Investigation, Formal Analysis, Data Curation, Writing – original draft. **Masoud Abedi:** Formal analysis, Investigation, Writing – original draft, Writing – review & editing

Data Availability

All data generated or analyzed during this study are included in this published article [and its additional files].

Ethical Approval

All animal experiments conducted in this study were reviewed and approved by the Research Ethics Committee of Shahid Bahonar University of Kerman, Kerman, Iran, ensuring compliance with ethical standards

Conflict of Interest

The authors declare that the research was conducted in the absence of any commercial or financial relationships that could be construed as a potential conflict of interest.

Consent for Publication

Not applicable.

Funding

This research was funded by a grant awarded by the Deputy of Research at Shahid Bahonar University of Kerman, Kerman, Iran

References

1. Iran R. The Chinkara *(Gazella bennettii*) in Iran, with the description of two new subspecies. *J Sci*. 1993; 4(3).
2. Ziaie H. A field guide to the mammals of Iran. Tehran: Department of the Environment; 1996.
3. Fadakar D, Malekian M, Hemami MR, Rezaei HR, Lerp H, Bärmann EV. Phylogenetic Assessment of *Gazella bennettii*: A Genetic Framework for the Conservation of the Endangered Jebeer in Iran. *Ecol Evol*. 2025; 15(2):e70954. https://doi.org/10.1002/ece3.70954
4. Mallon D, Kingswood S. Antelopes. Part 4: North Africa, the Middle East, and Asia. Global Survey and Regional Action Plans. SSC Antelope Specialist Group, IUCN, Gland, Switzerland and Cambridge, England. 2001.
5. Rahmani R, Izadi M, Khaledi B. Study on reproduction of Jebeer Gazelle (*Gazelle dorcas*) in Shir-Ahmad wildlife sancturary. 2004.
6. Sajjadian SM, Shojaei B, Molaei MM. Computed tomographic anatomy of the bronchial tree of the Jebeer Gazelle. *Iranian J Vet Surg*. 2008; (1):73-80. https://dor.isc.ac/dor/20.1001.1.20083033.2008.03.1.8.9
7. Shojaei B, Sajjadian S. Computed tomographic anatomy of the nasal cavity and paranasal sinuses of the jebeer. *Iranian J Vet Surg*. 2008; 3(4):75-84.
8. Diana A, Pivetta M, Cipone M. Imaging evaluation of the small animal mediastinum. *Vet Res Commun*. 2006; 30:145. https://doi.org/10.1007/s11259-006-0028-6
9. Prather AB, Berry CR, Thrall DE. Use of radiography in combination with computed tomography for the assessment of noncardiac thoracic disease in the dog and cat. *Vet Radiol Ultrasound*. 2005; 46(2):114-21. https://doi.org/10.1111/j.1740-8261.2005.00023.x
10. Greco A, Meomartino L, Gnudi G, Brunetti A, Di Giancamillo M. Imaging techniques in veterinary medicine. Part II: Computed tomography, magnetic resonance imaging, nuclear medicine. *Eur J Radiol Open*. 2023; 10:100467. https://doi.org/10.1016/j.ejro.2022.100467
11. Yoon J, Feeney DA, Cronk DE, Anderson KL, Ziegler LE. Computed tomographic evaluation of canine and feline mediastinal masses in 14 patients. *Vet Radiol Ultrasound*. 2004; 45(6):542-6. https://doi.org/10.1111/j.1740-8261.2004.04093.x
12. De Rycke LM, Gielen IM, Simoens PJ, van Bree H. Computed tomography and cross-sectional anatomy of the thorax in clinically normal dogs. *Am J Vet Res.* 2005; 66(3):512-24. https://doi.org/10.2460/ajvr.2005.66.512
13. Hahn KA, Lantz GC, Salisbury SK, Blevins WE, Widmer WR. Comparison of survey radiography with ultrasonography and x-ray computed tomography for clinical staging of subcutaneous neoplasms in dogs. *J Am Vet Med Assoc*. 1990; 196(11):1795-8.
14. Olby NJ, Müntana KR, Sharp NJ, Thrall DE. The computed tomographic appearance of acute thoracolumbar intervertebral disc herniations in dogs. *Vet Radiol Ultrasound*. 2000;41(5):396-402. https://doi.org/10.1111/j.1740-8261.2000.tb01860.x
15. Patsikas MN, Rallis T, Kladakis SE, Dessiris AK. Computed tomography diagnosis of isolated splenic torsion in a dog. *Vet Radiol Ultrasound*. 2001; 42(3):235-7. https://doi.org/10.1111/j.1740-8261.2001.tb00931.x
16. Henninger W. Use of computed tomography in the diseased feline thorax. *J Small Anim Pract*. 2003; 44(2):56-64. https://doi.org/10.1111/j.1748-5827.2003.tb00121.x
17. Takahashi A, Yamada K, Kishimoto M, Shimizu J, Maeda R. Computed tomography (CT) observation of pulmonary emboli caused by long-term administration of ivermectin in dogs experimentally infected with heartworms. *Vet Parasitol*. 2008; 155(3-4):242-8. https://doi.org/10.1016/j.vetpar.2008.04.027
18. Epperly E, Whitty JA. Equine imaging: computed tomography interpretation. *Vet Clin Equine Pract*. 2020; 36(3):527-43.
19. Pringle JK, Wojcinski ZW, Staempfli HR. Nasal papillary adenoma in a goat. *Can Vet J*. 1989; 30(12):964. https://pubmed.ncbi.nlm.nih.gov/17423479/
20. Gerros TC, Mattoon JS, Snyder SP. Use of computed tomography in the diagnosis of a cerebral abscess in a goat. *Vet Radiol Ultrasound*. 1998; 39(4):322-4. https://doi.org/10.1111/j.1740-8261.1998.tb01614.x
21. Di Giancamillo M, Lombardo R, Beretta S, Pravettoni D, Cipone M, Scanziani E, et al. Congenital facial infiltrative lipoma in a calf. *Vet Radiol Ultrasound*. 2002; 43(1):46-9. https://doi.org/10.1111/j.1740-8261.2002.tb00442.x
22. Alston C, Mengersen K, Gardner G. A new method for calculating the volume of primary tissue types in live sheep using computed tomography scanning. *Anim Prod Sci.* 2009; 49(11):1035-42. https://doi.org/10.1071/AN09038
23. Barnes H, Tucker RL, Grant BD, Roberts GD, Prades M. Lag screw stabilization of a cervical vertebral fracture by use of computed tomography in a horse. *J Am Vet Med Assoc.* 1995; 206(2):221-3.

24. Martens P, Ihler CF, Rennesund J. Detection of a radiographically occult fracture of the lateral palmar process of the distal phalanx in a horse using computed tomography. *Vet Radiol Ultrasound*. 1999; 40(4):346-9. https://doi.org/10.1111/j.1740-8261.1999.tb02122.x
25. Regodon S, Franco A, Garin J, Robina A, Lignereux Y. Computerized tomographic determination of the cranial volume of the dog applied to racial and sexual differentiation. *Cells Tissues Organs*. 1991; 142(4):347-50. https://doi.org/10.1159/000147214
26. Robina A, Regodón S, Guillen M, Lignereux Y. Utilization of computerized tomography for the determination of the volume of the cranial cavity of the Galgo Hound. *Cells Tissues Organs*. 1991; 140(2):108-11. https://doi.org/10.1159/000147044
27. Arencibia A, Vazquez J, Ramirez J, Sandoval J, Ramirez G, Sosa C. Anatomy of the cranioencephalic structures of the goat (Capra hircus L.) by imaging techniques: a computerized tomographic study. *Anat Histol Embryol*. 1997; 26(3):161-4. https://doi.org/10.1111/j.1439-0264.1997.tb00119.x
28. Walker NE, Olszewski ME, Wahle A, Nixon E, Sieren JP, Yang F, et al., editors. Measurement of coronary vasoreactivity in sheep using 64-slice multidetector computed tomography and 3-D segmentation. International Congress Series. Amsterdam: Elsevier Science; 2005. https://doi.org/10.1016/j.ics.2005.03.189
29. Shojaei B, Nazem MN, Vosough D. Anatomic reference for computed tomography of the paranasal sinuses and their openings in the Rayini goat. *Iranian Journal of Veterinary Surgery*. 2008; 3(2):77-85.
30. Onar V, Kahvecioglu K, Çebi V. Computed tomographic analysis of the cranial cavity and neurocranium in the German shepherd dog (Alsatian) puppies. *Vet Arh*. 2002; 72(2):57-66.
31. Cardoso L, Gil F, Ramírez G, Teixeira M, Agut A, Rivero M, et al. Computed tomography (CT) of the lungs of the dog using a helical CT scanner, intravenous iodine contrast medium and different CT windows. *Anat Histol Embryol*. 2007; 36(5):328-31. https://doi.org/10.1111/j.1439-0264.2007.00776.x
32. Smallwood JE, George TF. Anatomic atlas for computed tomography in the mesaticephalic dog: thorax and cranial abdomen. *Vet Radiol Ultrasound*. 1993; 34(2):65-84. https://doi.org/10.1111/j.1740-8261.1993.tb01510.x
33. Shojaei B, Vajhi A, Rostami A, Molaei M, Arashian I, Hashemnia S. Computed tomographic anatomy of the abdominal region of cat. *Iran J Vet Res*. 2006; 7(2):45-52.
34. Shojaei B, Rostami A, Vajhi A, Shafaee M. Computed tomographic anatomy of the thoracic region of the cat. *Vet Arh*. 2003; 73(5):261-70.
35. Vladova D, Stefanov M, Toneva Y. Computed tomography study of thoracic aorta in the cat. *Bulg J Vet Med*. 2005; 8(3):151–6.
36. Vladova DI, Toneva YG, Stefanov M. Computed tomography (CT) of the cranial mediastinum in the cat (Felis silvestris f. domestica). *Trakia J Sci*. 2005; 3(1):53-7.
37. Samii VF, Biller DS, Koblik PD. Normal cross-sectional anatomy of the feline thorax and abdomen: comparison of computed tomography and cadaver anatomy. *Vet Radiol Ultrasound*. 1998; 39(6):504-11. https://doi.org/10.1111/j.1740-8261.1998.tb01640.x
38. Braun U, Irmer M, Augsburger H, Jud R, Ohlerth S. Computed tomography of the abdomen in Saanen goats: I. Reticulum, rumen and omasum. *Schweiz Arch Tierheilkd*. 2011; 153(7):307-13. https://doi.org/10.5167/uzh-49065
39. Ohlerth S, Becker-Birck M, Augsburger H, Jud R, Makara M, Braun U. Computed tomography measurements of thoracic structures in 26 clinically normal goats. *Res Vet Sci*. 2012; 92(1):7-12. https://doi.org/10.1016/j.rvsc.2010.10.019
40. Alsafy M. Computed tomography and cross-sectional anatomy of the thorax of goat. *Small Rumin Res*. 2008; 79(2-3):158-66. https://doi.org/10.1016/j.smallrumres.2008.07.028
41. Sajjadian SM, Shojaei B, Sohrab Zade B. Computed Tomographic Anatomy of the Abdominal Cavity in the Jebeer (*Gazella bennettii*). *Anat Sci* J. 2015; 12(1):37-44.
42. Shojaei B, Vosough D, Sharifi F. Computed tomographic anatomy of the thoracic cavity vessels in the rayini goat. *Iran J Vet Surg*. 2012; 7(1-2):9-22. https://dor.isc.ac/dor/20.1001.1.20083033.2012.07.1.1.0
43. Sisson S. The anatomy of the domestic animals. Philadelphia: WB Saunders Company; 1975.
44. Done SH, Ashdown RR. Color atlas of veterinary anatomy. Elsevier; 2011.